pubs.acs.org/acschemicalbiology

Articles

Controlled Protein Activities with Viral Proteases, Antiviral Peptides, and Antiviral Drugs

Elliot P. Tague, Jeffrey B. McMahan, Nathan Tague, Mary J. Dunlop, and John T. Ngo*

Cite This: *ACS Chem. Biol.* 2023, 18, 1228−1236

Read Online

ACCESS | Metrics & More | Article Recommendations | Supporting Information

ABSTRACT: Chemical control of protein activity is a powerful tool for scientific study, synthetic biology, and cell therapy; however, for broad use, effective chemical inducer systems must minimally crosstalk with endogenous processes and exhibit desirable drug delivery properties. Accordingly, the drug-controllable proteolytic activity of hepatitis C *cis*-protease NS3 and its associated antiviral drugs have been used to regulate protein activity and gene modulation. These tools advantageously exploit non-eukaryotic and non-prokaryotic proteins and clinically approved inhibitors. Here, we expand the toolkit by utilizing catalytically inactive NS3 protease as a high affinity binder to genetically encoded, antiviral peptides. Through our approach, we create NS3-peptide complexes that can be displaced by FDA-approved drugs to modulate transcription, cell signaling, and split-protein complementation. With our developed system, we invented a new mechanism to allosterically regulate Cre recombinase. Allosteric Cre regulation with NS3 ligands enables orthogonal recombination tools in eukaryotic cells and functions in divergent organisms to control prokaryotic recombinase activity.

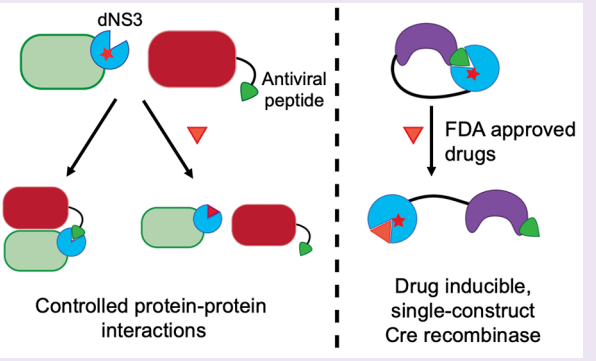

INTRODUCTION

The ability to tune and dynamically control protein activity empowers the study of biological phenomena, engineering of synthetic biology, and design of safer cellular therapies. To achieve protein activity control, small molecules are particularly useful because they can be dose-dependent, dynamic, and delivered through multiple administration routes. Prominent examples of such ligand-dependent methods to control protein activity include chemically induced protein proximity (CIPP),[1−5] induced protein trafficking,[6] and controlled enzymatic activity.[7] However, small molecules used in this context often exhibit endogenous crosstalk in mammalian organisms and the human microbiome, or they exhibit poor bioavailability.

For synthetic biology and future therapeutic applications, an ideal ligand inducible system would be orthogonal to eukaryotic and prokaryotic biology, present at low levels in the environment, versatile, tunable, and dynamic. To employ more orthogonal inducers and build upon the library of existing chemogenetic proteins, we and others developed the ligand inducible connection (LInC) system and stabilizable polypeptide linkages (StaPLs), which utilize hepatitis C virus (HCV) *cis*-protease NS3 and its host of clinically tested antiviral drugs.[8,9] These systems facilitate control of transcription, protein localization, and cell signaling by utilizing highly specific and characterized ligands developed to bind a nonendogenous target protein.

Yet, an expanded repertoire of ligands exists to inhibit NS3, each with potential value as a synthetic biology tool. Due to the essential function of NS3 in viral replication, multiple approaches have been employed to develop NS3 inhibitor ligands, including genetically encodable ligands such as RNA aptamers and peptides.[10,11] Recent applications utilize NS3 and genetically encoded antiviral peptides to control various protein functions.[12−15] In this schema, NS3 protease serves as a high affinity binder to antiviral peptides, which can be conditionally displaced by small molecule drugs.

Since NS3 in this context serves as a high affinity binder instead of a severable linker, the protease no longer needs to be catalytically active. Although NS3 protease exhibits stringent substrate specificity,[16] there are documented endogenous cleavage sites involved in viral immune response[17,18] and some recently discovered promiscuity in the cleavage sequence.[19] Thus, the ablation of NS3 proteolytic capacity can now be applied to improve the orthogonality of chemosensory tools used for control of protein function.

Received: March 6, 2023
Revised: April 13, 2023
Accepted: April 25, 2023
Published: May 4, 2023

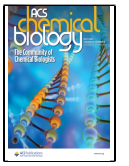

https://doi.org/10.1021/acschembio.3c00138
ACS Chem. Biol. 2023, 18, 1228−1236

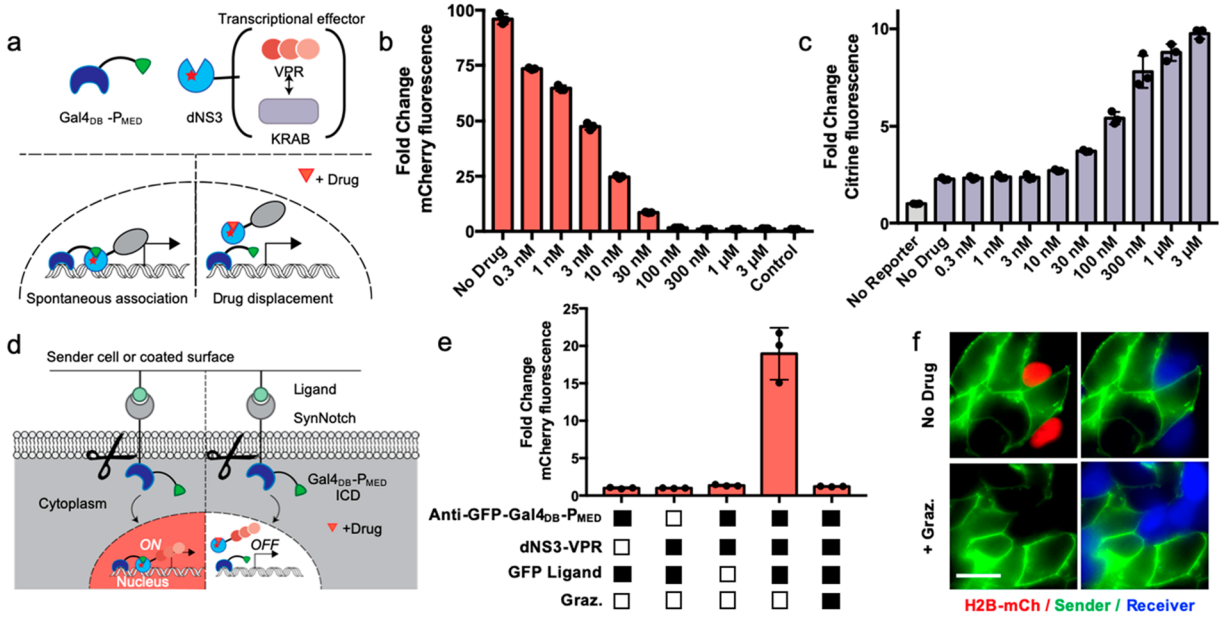

Figure 1. Antiviral drug control of transcriptional effectors and cell signaling (a) $Gal4_{DB}$-P_{MED} complexes with dNS3-fused transcriptional effectors, creating heterodimeric transcription factors that can be competitively inhibited by antiviral drugs. (b) Transcriptional turn-off of Gal4 driven H2B-mCherry expression in HEK293FT cells via competitive grazoprevir inhibition of dNS3−VPR binding to $Gal4_{DB}$-P_{MED}. (c) Drug control of UAS-CMV-H2B-citrine expression via competitive grazoprevir inhibition of repressor domain dNS3−KRAB binding to $Gal4_{DB}$-P_{MED}. (d) Design of drug-controlled Notch ICD function. $Gal4_{DB}$-P_{MED} drives expression in the presence of a receptor ligand, dNS3-VPR, and the absence of a drug. (e) Combinatorial control of UAS-H2B-mCherry expression via surface coated ligand GFP and drug-controlled displacement of dNS3-VPR from $Gal4_{DB}$-P_{MED} ICD. (f) Drug controlled transcription via ligand mediated release of SynNotch $Gal4_{DB}$-P_{MED} ICD in dual HEK293FT coculture. Sender cells are expressing a surface presented GFP ligand, and the receiver cell contains transiently expressed SynNotch $Gal4_{DB}$-P_{MED} and dNS3-VPR to drive the UAS-H2B-mCherry reporter. Receiver cells express iRFP670 (false colored blue) for labeling purposes. Scale bar: 20 μm. All quantitative fluorescent data were captured via flow cytometry of transiently transfected HEK293FT cells, 48 h post-transfection/drug addition aside from UAS-H2B-mCherry, which was clonally incorporated into HEK293FT. Plotted values are the mean ± SD of biologically independent replicates, n = 3. Unless otherwise stated, drug refers to 3 μM grazoprevir.

In this work, we chemically control protein functions using catalytically inactivated or drug-resistant NS3 mutants paired with displaceable, genetically encoded peptides. Through this approach, we expand the utility of antiviral drugs to conditionally regulate transcription, cell signaling, split-protein complementation, and intramolecular inhibition. With our approach, we discover a novel single-chain mechanism to control Cre recombinase with applicability across eukaryotic and prokaryotic domains. Lastly, we discover that specific drug-resistance mutations employed in the proteolytic NS3 tools[9] extend to peptide displacement tools. We use these properties to create combinatorial drug control of Cre recombinase.

RESULTS

Controlled Transcription and Cell Signaling. To first validate our approach, we devised a system to control the assembly of heterodimeric transcription factors with antiviral drugs. We began by fusing a previously developed high affinity antiviral peptide (CP5-46A-4D5E, referred to here as P_{MED})[11] to the Gal4 DNA-binding domain ($Gal4_{DB}$) and then fused a separate catalytically "dead" $NS3^{S139A}$ serine protease (dNS3) to a transcriptional effector domain (Figure 1a). In the absence of the drug, the antiviral peptide and dNS3 are expected to spontaneously assemble to form a functional synthetic transcription factor. Upon the addition of a small molecule drug, dNS3 is expected to competitively bind to the drug over the peptide, therefore inhibiting the activity of the transcriptional effector.

To first mediate transcriptional activity, transcriptional activator VPR[20] was fused to dNS3. In this configuration, we expected spontaneous association between the $Gal4_{DB}$-peptide and dNS3-VPR to lead to transcriptional activation and drug addition to lead to transcriptional shut-off. Correspondingly, we transiently transfected $Gal4_{DB}$-peptide and dNS3-VPR and observed spontaneous transcriptional activation of a genomically integrated UAS-H2B-mCherry reporter in HEK293 cells (Figure 1b). As we increased the concentration of the NS3 inhibitor grazoprevir, we observed dose dependent transcriptional inhibition with a near 100-fold range of protein expression. We tested two peptides developed against $NS3^{WT}$ by Kügler et al.—medium affinity CP5-46A-4D5E and high affinity CP5-46-4D5E, referred to here as P_{MED} and P_{HI}, respectively (Table S1). Interestingly, P_{HI} fused to $Gal4_{DB}$ acted as a transcriptional activation domain even in the absence of dNS3-VPR cotransfection, while $Gal4_{DB}$-P_{MED} displayed no observable activation on its own (Figure S1). The P_{HI} sequence contains features that are consistent with that of many known ADs, including an enrichment of acidic, aliphatic, and aromatic side chains[21] (see Table S1 for sequence). Consequently, only P_{MED} was used for the transcriptional effector work while P_{HI} was reserved for future, nontranscriptional applications. We next predicted that the effector domain could be exchanged to control contrasting transcriptional outputs. To test this, we fused dNS3 to transcriptional repressing domain KRAB to control transcriptional repression of a constitutive reporter gene, UAS-CMV-H2B-Citrine (Figure 1c). As expected, transcriptional

https://doi.org/10.1021/acschembio.3c00138
ACS Chem. Biol. 2023, 18, 1228−1236

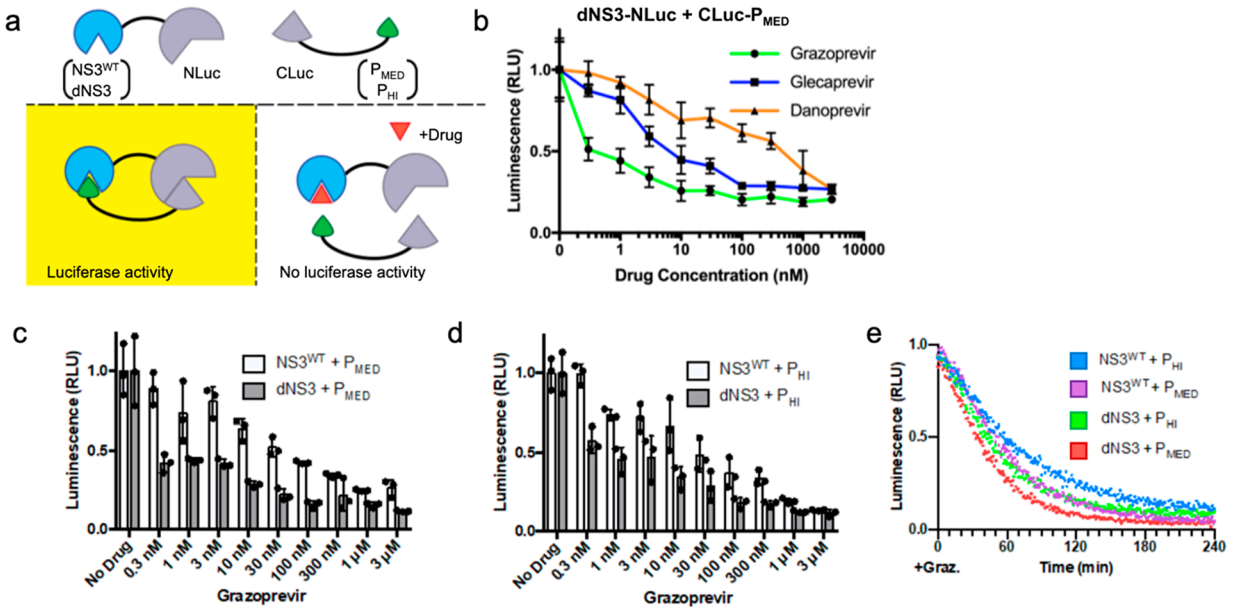

Figure 2. Split luciferase control and drug dissociation characterization. (a) Design of split luciferase constructs. NLuc(12−1247) was fused to dNS3 or $NS3^{WT}$. CLuc(1200−1643) was fused to P_{MED} or P_{HI} peptide. (b) Dose response of HEK293FT cells transfected with dNS3-NLuc and CLuc-P_{MED} to various drugs. Lines are connected to guide the eye. (c) Dose response of NLuc fused to $NS3^{WT}$ or dNS3 in combination with CLuc fused to P_{MED} or (d) higher affinity P_{HI} (e). Temporal response to the drug of the four different combinations of NLuc and CLuc fusions to NS3 and peptides. All dose responses are normalized to their respective no drug controls and transfected 48 h before lysing for luciferase experiments. The drug was added at the time of transfection for dose response experiments. For temporal experiments, 3 μM of grazoprevir was added at the time of lysis. Plotted values are the mean ± SD of biologically independent replicates, n = 3. For linear regression and SD of Figure 2e, see the Supporting Information.

repression occurred in the absence of the drug up to 8-fold, and the extent of repression could be controlled by altering the concentration of grazoprevir.

These transcriptional effectors can also govern programmable cell signaling. To demonstrate this, we sought to apply drug-dependent transcriptional control in tandem with SynNotch cell signaling. SynNotch represents a highly modular approach to sense an extracellular ligand and proteolytically trigger the release of an intracellular domain (ICD). In practice, this customizable cell signaling platform has been used to create multicellular patterning as well as combinatorial antigen-sensing circuits to combat cancer.[22,23] Drug control of SynNotch would enable the creation of more complex gene circuits and safety switch behavior for therapeutic applications. For these reasons, we replaced the ICD of a previously developed Anti-GFP SynNotch[22] with our $Gal4_{DB}$-P_{MED} (Figure 1d). In this arrangement, gene activation is controlled by extracellular ligand induced proteolysis and drug-controlled docking of dNS3-VPR, with the goal of allowing for tight combinatorial control of ICD transcriptional activation of SynNotch.

Cells containing the modified SynNotch constructs were grown on surfaces coated with GFP ligand in the presence of varying grazoprevir concentrations. When the ligand was presented in the absence of the drug, HEK293 cells exhibited UAS-H2B-mCherry reporter activation, while increasing concentration of the drug led to dose-dependent transcriptional inhibition (Figure 1e, Figure S2a). Due to an extracellular c-Myc epitope tag, transcription could also be controlled by plated c-Myc antibody ligands (Figure S2b). Small molecule control of SynNotch additionally extended to the application of intercellular signaling, which we tested by creating a GFP surface ligand "sender" cell line and then cocultured these cells with transiently transfected dNS3/peptide SynNotch "receiver" cells. Cocultured receiver cells exhibited drug-dependent transcriptional turn-off when presented with the GFP ligand (Figure 1f, Figure S2c).

Controlled Enzymatic Activity by Split Protein Complementation. We next examined the binding characteristics of drug-controlled complementation with the goal of directly demonstrating drug-mediated dissociation of formed NS3−peptide complexes. Since dNS3 and its high affinity peptides effectively regulated assembly of a split transcription factor, we surmised that dNS3/peptide complementation could control the assembly of a split protein to control enzymatic activity. To test this, we fused permutations of dNS3, $NS3^{WT}$, and each peptide variant to split fragments of *Renilla* luciferase (Figure 2a). Controlled assembly of split luciferase not only demonstrates control of enzyme activity but it can also be used to elucidate binding characteristics through dynamic luciferase complementation assays.[24]

We first turned to the previously identified set of dNS3 and P_{MED} as our model peptide docking pair and tested luciferase activity in transfected HEK293 lysates upon the addition of four different drugs: grazoprevir, glecaprevir, danoprevir, and telaprevir (Figure 2b, Figure S3). The first three of these drugs inhibit luciferase activity in a dose dependent manner, representing multiple ligand choices with distinct binding profiles. However, split luciferase constructs containing dNS3 exhibit significant resistance to telaprevir. This observation is consistent with the drug's covalent binding mechanism to the catalytic Ser139,[25,26] which is mutated in dNS3, and this effect is reverted upon replacement with wild-type NS3 (Figure S3).

Since NS3's catalytic serine residue could affect binding characteristics, we tested both $NS3^{WT}$ and dNS3 with P_{MED} and P_{HI} peptides as fusions to split luciferase subunits. All

https://doi.org/10.1021/acschembio.3c00138
ACS Chem. Biol. 2023, 18, 1228−1236

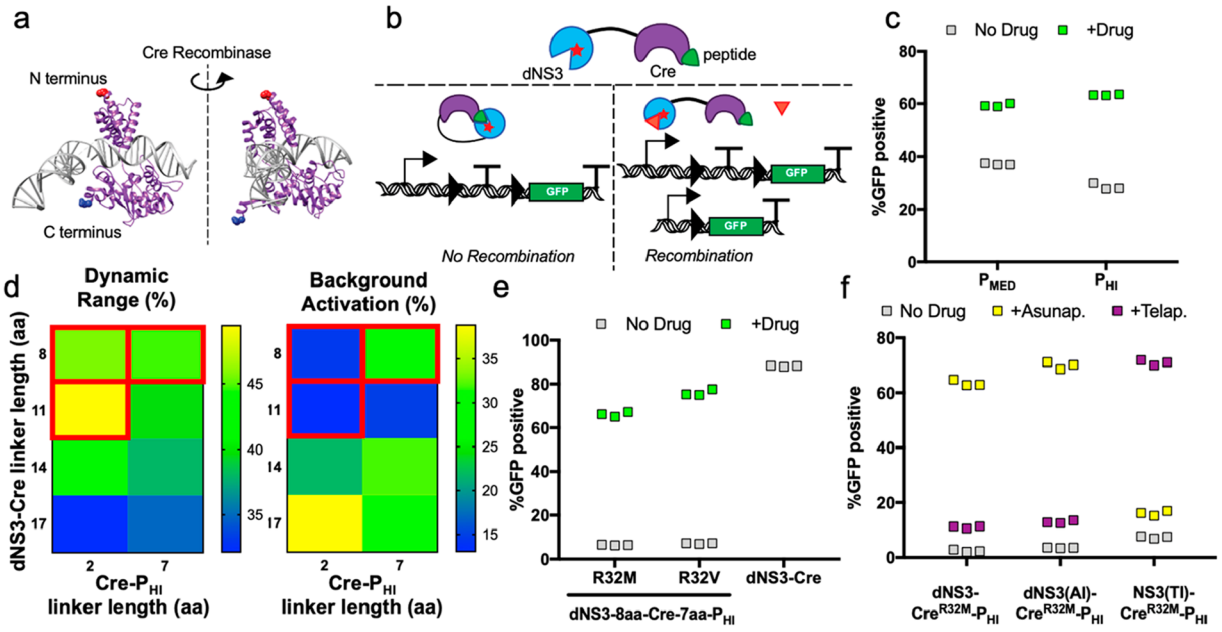

Figure 3. Antiviral drug control of genetic recombination in eukaryotes. (a) Structure of Cre recombinase bound to DNA (PDB 1ma7[28]). N-terminal and C-terminal residues labeled in red and blue, respectively. (b) Design of intramolecular inhibited Cre mediating drug-dependent recombination of a virally-integrated Cre reporter gene. Successful recombination results in GFP expression after excision of a stop codon. (c) Comparison of transient transfection of dNS3-Cre-peptide with P_{MED} and P_{HI} with flow cytometry, 48 h post-transfection and drug addition in HEK293FT cells. (d) Variation of amino acid (aa) linkers between dNS3-Cre and Cre-P_{HI} with flow cytometry, 48 h post-transfection and drug addition. Constructs chosen for highest dynamic range of GFP positive cells upon addition of the drug and for a low background of GFP positive cells in the absence of a drug. Optimal linker lengths are boxed in red. (e) dNS3-Cre-P_{HI} variants with selected Cre mutants compared against dNS3-Cre control. (f) Selectivity of drug resistant NS3-Cre-P_{HI} constructs against asunaprevir (1 μM) and telaprevir (10 μM). The drug was added 24 h post-transfection, and flow cytometry data were collected 48 h postdrug addition. Unless otherwise specified, drug refers to 1 μM grazoprevir addition. Plotted values are biologically independent replicates, n = 3.

permutations of these constructs were functionally sensitive to the range of grazoprevir concentrations we tested (Figure 2c,d). Notably, the split luciferase heteromerized by dNS3 displays slightly increased sensitivity to the drug than $NS3^{WT}$ does, possibly due to the loss of a hydrogen bond between the peptides and NS3 as a result of the S139A mutation. However, the affinity differences of the two peptides tested did not seem to make a substantial difference in dose response to grazoprevir at the concentrations tested (Figure S4a,b).

We next demonstrated the temporal displacement of peptide by taking advantage of the reversibility of split luciferase complementation. Temporal dissociation of proteins is important for many biological processes and is often desired for dynamic protein activity control. Kinetics of displacement were measured over a 4 h period with excess drug concentration and normalized to their respective no drug controls (Figure 2e, Figure S5a,b). In this configuration, the fusions of dNS3 and P_{MED} to split luciferase yielded the fastest displacement kinetics, with luciferase activity reduced to half maximal activity at ~30 min. The replacement of dNS3 with $NS3^{WT}$ or the replacement of P_{MED} with P_{HI} increased the time to displacement, reflecting expected increases in protein-peptide affinity. Following peptide and NS3 variations, we tested multiple drugs with dNS3 and P_{MED} (Figure S6a,b) but observed little difference in dissociation rate at saturating drug concentrations aside from telaprevir, which did not dissociate dNS3−P_{MED} complexes well. Altogether, the classes of previously developed peptides and small molecules allow for variation of binding kinetics and dose responses with multiple antiviral drugs. Temporal experiments additionally reveal that antiviral drugs can disrupt preformed protein−peptide complexes.

Controlled Genetic Recombination through Intramolecular Inhibition. Disruption of preformed protein−peptide complexes led us to hypothesize that we could control intramolecular protein interactions, i.e., engineer synthetic protein allostery. In native biology, enzymes are routinely controlled by allosteric mechanisms. Synthetic protein allostery is advantageous in a biological tool because it offers a self-encoded mechanism of control, and it can expand the utility of a protein tool across organisms. To demonstrate these capabilities, we next sought to allosterically control enzyme activity via dNS3 and an inhibitory peptide.

For this application, we focused on Cre recombinase because it is a widely used enzyme that often requires ligand control. Cre recombinase is a site specific DNA recombinase that has been traditionally controlled by conditional nuclear translocation via 4-hydroxytamoxifen[7] or various split protein complementations.[27] Yet, Cre is commonly used in developmental biology studies, which often require genetically small constructs for viral incorporation and orthogonal inducer ligands that are sparsely present in the environment. For these types of applications, we instead envisioned a single construct, drug-inducible Cre controlled by antiviral drugs. Cre is a tyrosine recombinase, and since no available unbound Cre structures existed, we compared the structure of bound Cre (Figure 3a) to related unbound and bound tyrosine recombinases such as XerA and XerD.[28,29] Comparisons reveal that each of these tyrosine recombinases forms a C-shaped clamp composed of two domains, separated by a flexible linker.

https://doi.org/10.1021/acschembio.3c00138
ACS Chem. Biol. 2023, 18, 1228−1236

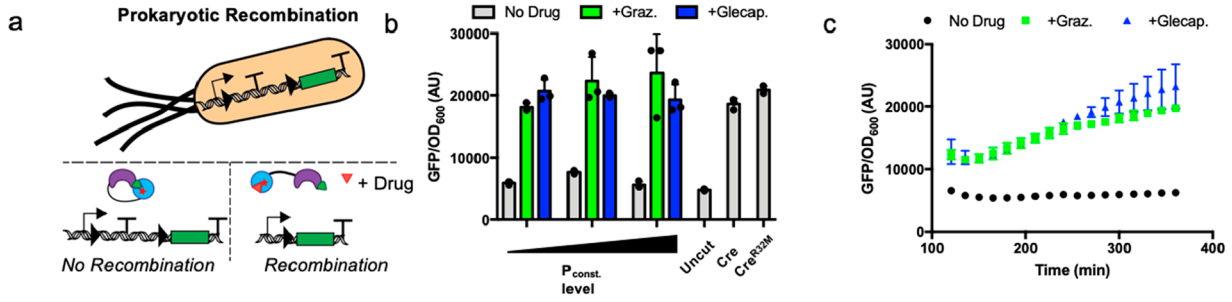

Figure 4. Drug control of genetic recombination in prokaryotes. (a) Genetic recombination in prokaryotes. To report on Cre mediated recombination, a transcriptional terminator is located after a constitutive promoter and excised by Cre recombination. (b) Constitutively expressed dNS3-Cre^{R32M} -P_{HI} in *E. coli* with no drug treatment compared to 50 μM of grazoprevir or glecaprevir treatment, 6 h post drug addition, fluorescence/OD_{600} quantified by the plate reader. Three constitutive promoters ($P_{const.}$) were tested with low to medium level expression. These inducible Cre constructs are compared to less expressed constitutive Cre and Cre^{R32M}. (c) Time course response of dNS3-Cre^{R32M} -P_{HI} in *E. coli* during exponential growth with and without drug treatment (50 μM, added at time 0). Values are shown starting after 120 min due to low OD_{600} prior to this timepoint. Values shown are fluorescence (a.u., superfolder GFP) normalized to cell density (OD_{600}), mean ± SD, n = 3 biologically independent replicates.

Furthermore, recent studies of Cre recombinase demonstrate independent folding mechanisms of the two N- and C-terminal domains.[30] Based on these observations, we inferred that Cre undergoes a large conformational change to regulate DNA cleavage and hypothesized that the fusion of dNS3 and an inhibitory peptide at opposing termini of Cre could result in drug controlled intramolecular occlusion of the enzyme (Figure 3b). To measure drug-inducible dNS3-Cre-peptide recombination, all constructs were tested in a clonal Cre-stoplight reporter HEK293 cell line in which Cre activity results in constitutive GFP expression. Initial testing with the P_{MED} peptide revealed promising results, and dynamic range improved with replacement of P_{MED} with higher affinity P_{HI} (Figure 3c).

Recombination modulates expression of GFP with a binary DNA excision event, making it crucial to reduce basal recombination in the absence of drug. Following substitution of P_{MED} with P_{HI}, we began further optimization for lower background recombination while retaining high dynamic range. To further reduce basal recombination, flexible amino acid (aa) linker length was varied between the N-terminal fusion of dNS3 to Cre and between the C-terminal fusion of P_{HI} to Cre (Figure 3d). From the linker variations tested, we chose three candidates with high dynamic range of activation upon grazoprevir addition and low background activation in absence of drug (Figure 3d, boxed in red).

Before moving forward with these three selected linker variants, we noted that there was still significant background activation, which we aimed to reduce with further optimization. We hypothesized that some intramolecular dNS3 and P_{HI} interactions were spontaneously active, subsequently allowing these Cre molecules to cooperatively dimerize through native Cre termini interactions.[31,32] To mitigate cooperativity and decrease background, we next mutated the Cre *R*32 site, which is thought to decrease cooperativity and has been shown to increase recombination accuracy.[33] This mutation choice is further supported by recent development to control Cre with light inducible AsLOV2 and destabilizing N- and C-terminal Cre mutations (coined LiCre).[34] The Cre^{R32M} mutation caused a considerable decrease in background for all dNS3-Cre-P_{HI} constructs tested in transient transfection (Figure S7a), and linker variant dNS3-8aa-Cre^{R32M}-7aa-P_{HI} provided optimally low background recombination and high dynamic range. This linker variant exhibited favorable properties with either Cre^{R32M} or similarly reported Cre$^{R32\ V}$ mutations, suggesting that this mutation site results in a drug inducible Cre with minimal background in addition to its previously characterized higher accuracy of recombination (Figure 3e, Figure S7b–d). The percentage of recombination-positive cells increased ∼70% upon addition of the drug. Each of these final inducible Cre constructs activated a similar fraction of cells compared to their Cre^{WT} counterparts, while the dNS3-Cre^{WT} control remained constitutively active (Figure S7c,d).

Equipped with an optimized inducible Cre system, we explored opportunities to control genetic recombination in two different cell populations to reflect the higher complexity of gene expression in specific cell lineages. To accomplish this, we sought to make orthogonal inducible Cre recombinases. In previous work, Jacobs et al. demonstrated that specific mutations to active NS3 protease could create drug resistant orthogonal protease pairs that are asunaprevir inducible (AI) or telaprevir inducible (TI).[9] We hypothesized that the antiviral peptides would retain reasonable affinity to mutated NS3 proteases due to the large surface area that peptides bind on NS3, and subsequently these NS3 mutants could be used in our NS3-peptide control systems. Introducing these protease mutants into our peptide-based inducible Cre system led to a new pair of orthogonal Cre constructs that can be strongly induced via asunaprevir or telaprevir with low background recombination (Figure 3f and Figure S8a,b). Alternatively, the original catalytic NS3^{S139A} mutation is also sufficient on its own to reduce telaprevir sensitivity while retaining asunaprevir induction (Figure 3f), consistent with previous experimental results (Figure S3). Applying the NS3^{S139A} mutation to the NS3(TI) similarly ablates telaprevir sensitivity, leaving only sensitivity to grazoprevir among the three drugs tested here (Figure S8). Collectively, these inducible Cre recombinases can respond to two distinct antiviral drugs and also demonstrate a mechanism of covalent ligand control of enzymatic activity that can be reversed with catalytically inactive NS3.

Last, we recognized that drug-controlled recombination with a single-chain Cre construct could potentially translate across divergent organisms. Given our engineered control mechanism of Cre does not rely on nuclear translocation and instead relies

https://doi.org/10.1021/acschembio.3c00138
ACS Chem. Biol. 2023, 18, 1228−1236

on allosteric control (Figure S9), we expected antiviral drug inducible Cre to be highly versatile across organisms and function in prokaryotes. To test this, we cotransformed dNS3-Cre^{R32M}-P_{HI} and the GFP Cre reporter into *Escherichia coli* (Figure 4a). Cre constructs were expressed at a constant level under an arabinose inducible promoter (Figure S10a) or under a broad range of constitutive expression levels (Figure 4b, Table S2). Upon induction with antiviral drugs, GFP expression significantly increased, with detectable GFP expression occurring at <120 min under a constitutive promoter (Figure 4c) and no significant change to bacterial growth (Figure S10b,c). We observed minimal background recombination via dNS3-Cre^{R32M}-P_{HI} in the absence of the drug, while in contrast, both dNS3-Cre^{R32M} lacking inhibitory peptide and Cre^{R32M} exhibited substantial recombination. The dNS3-Cre^{R32M} and Cre^{R32M} background recombination could not be remedied even under an uninduced, arabinose-driven promoter (Figure S10a). Interestingly, drug concentrations of antiviral drug inducible Cre needed to be increased from the levels used in mammalian cells, consistent with previous literature utilizing HCV NS3 in bacteria.[35,36] Nevertheless, maximal recombination occurred as low as 6.25 μM of glecaprevir or grazoprevir (Figure S11). Overall, this tool enables drug inducible recombination in prokaryotic cells and mammalian cells with chemical inducers that are minimally toxic to both cell types.

DISCUSSION

In this study, we demonstrate diverse controls over protein activity via dNS3, genetically encoded inhibitory peptides, and highly characterized antiviral drugs. To this end, we show antiviral drug regulation of transcriptional complex formation, cell signaling, split enzyme domains, and synthetic allostery of Cre recombinase.

Analysis of peptide binding characteristics revealed tunable and dynamic control of protein−protein interaction, and this system can respond to a myriad of different drugs. Dose responses of these systems can also be tuned via swapping genetic parts such as peptides, alternate forms of NS3, or by the specific drug used. These features underscore the benefits to using a highly characterized target such as NS3 as a synthetic tool. Due to the diversity of approaches to target NS3, high affinity, bioavailable small molecule drugs can be paired with alternate inhibitors such as genetically encoded peptides. Furthermore, the effort to develop ligands against NS3 is ongoing,[37] with FDA approvals of molecules such as glecaprevir as recently as 2017, providing researchers a continually expanding toolkit to control these protein tools synthetically.

Alongside our demonstration of the versatility of NS3 and its associated inhibitors, we devised a new mechanism to allosterically control Cre recombinase through structure-guided design. This system displayed the ideal characteristics of low background recombination and high dynamic range while utilizing orthogonal ligands and a single optimized protein. Extensive clinical efforts to develop NS3 inhibition enabled us to expand the repertoire of Cre recombinase tools as well. Building upon characterization of drug-resistant mutants and proteolytic tools,[9] we extended drug-resistant NS3 mutants to control peptide binding with two orthogonal, FDA approved inhibitors.

Last, allosterically controlled Cre and antiviral drug inducers easily transferred across domains of life to function in *E. coli*. Minimal toxicity to prokaryotic and eukaryotic hosts opens up greater possibilities of studying causal roles of microbiome gene expression *in vivo* as well as engineering industrial bacterial processes. In contrast to many available bacterial chemical inducers, NS3 inhibitors are not known metabolites of bacterial cells, which increases ligand orthogonality for future microbiome applications. In future work, expression of randomly mutated versions of the engineered Cre may enable further optimization of the construct via directed evolution using iterative or continuous screening techniques.

In contrast to our previously developed LInC system, the currently presented tools offer new methods to control protein−protein complementation and synthetic allostery through a catalytically inactive protease. The LInC system is composed of chimeric proteins with domain linkages that are conditionally preserved in the presence of drug, whereas the system here allows for proteins or protein domains to be displaced from one another in the presence of the drug. These two approaches can exist in parallel, and future toolmakers will be able to evaluate which method is more appropriate to use on a case-by-case basis. As a whole, NS3 and its associated inhibitors represent an exciting toolkit to control protein activity in a more orthogonal manner for eukaryotic and prokaryotic organisms.

METHODS

DNA Constructs. Standard procedures of ligation and Gibson assembly were applied to all constructs created for this paper. The Cre reporter plasmid (Addgene #62732) was a gift from Niels Geijsen (Hubrecht Institute). The eGFP-pBAD plasmid (Addgene #54762) was a gift from Michael Davidson (Florida State University), and the pmiRFP670-N1plasmid (Addgene #79987) was a gift from Vladislav Verkhusha (Albert Einstein College of Medicine). See the Supporting Information for annotated DNA sequences used in this work.

Mammalian Cell Culture. HEK293FT cells were purchased from Thermo Fisher and maintained in a 37 °C incubator with 5% CO_2. Cells were cultured in high-glucose DMEM containing 10% FBS and supplemented with nonessential amino acids (Life Technologies) and Glutamax (Life Technologies). For UAS-H2B-mCherry experiments, a clonal cell line was previously created via random plasmid insertion followed by drug selection and single clone isolation. Individual clones were chosen for use based on their low background expression and high inducibility of reporter gene upon transfection with a plasmid encoding Gal4-VP64. Cells containing the integrated reporter DNA were selected with Zeocin (100 μg/mL, Invivogen). For generation of a Cre reporter line, the lentiviral Cre reporter plasmid (62732) was modified to have blasticidin resistance. This construct was then virally transduced and selected for with blasticidin (10 μg/mL, Invivogen) and a single clone was isolated by limited dilution into 96 well plates clonally selected by serial dilution. Individual reporter line clones were chosen for use based on high recombination using wild type, unfused Cre recombinase.

DNA Transfections and NS3 Inhibitors. All DNA transfections were carried out using Lipofectamine 3000 (Thermo Fisher) according to the manufacturer's instructions. All transcriptional effector experiments were carried out at a mass ratio between 1:2 and 1:3 of $Gal4_{DB}$ constructs to the transcriptional effector. For imaging experiments, fibronectin (Product #F1141, Sigma-Aldrich) was seeded on to glass coverslip substrate at a dilution of 5 μg/mL for 1 h at RT and rinsed three times with PBS before seeding cells. All other experiments were carried out on tissue cultured treated plastic (Corning) or for cell adherence by the manufacturer (ibiTreat by Ibidi).

The drug was either added at the time of transfection or 24 h later. Grazoprevir, danoprevir, telaprevir, and glecaprevir were purchased from MedChemExpress. Stocks were prepared at between 3 -10 mM concentrations between 3 and 10 mM by dissolution in DMSO.

https://doi.org/10.1021/acschembio.3c00138
ACS Chem. Biol. 2023, 18, 1228−1236

Protein Purification. The GFP SynNotch ligand was expressed and purified from *E. coli* DH10B cells (Thermo Fisher). *E. coli* was transformed with arabinose inducible EGFP-pBAD plasmid (Addgene #54762) overnight at 37 °C. The following day, the bacterial An overnight starter culture was diluted 1:50 into 0.5 L of LB and was grown at 37 °C with shaking until an OD_{600} of 0.8 was reached, at which point the culture was cooled to 25 °C and GFP expression was induced by the addition of arabinose to a final concentration of 0.02% (w/v). Expression proceeded for 24 h at 25 °C with agitation (250 rpm). Cells were pelleted at 3000 rcf and the His-tagged GFP was purified using the QiaExpress Ni-NTA Fast Start protein purification kit (Qiagen, Catalog # 30600) under native conditions.

Ligand Coating and Coculture for SynNotch Experiments. For plated ligand experiments, untreated tissue culture plastic was incubated with purified GFP (diluted to 18 μg/mL) or c-Myc Monoclonal Antibody (Invitrogen 9E10.3, Catalog #AHO0062, diluted to 1 μg/mL) in PBS for 1 h at RT. Plates were subsequently washed three times with PBS prior to adding transfected cells and the drug being mixed in cell culture media.

For coculture experiments, sender cells were virally transduced with constitutive surface-presenting GFP-ligand and allowed to grow for 2 days. Lentivirus was prepared via transient transduction of the GFP-ligand construct, VSVG, and PAX2 packaging plasmids for 6−12 h before removing transfection media. After 24 and 48 h, media was collected and replaced. The supernatant was then filtered with 0.45 μM sterile filters (Whatman, Catalog #6780−2504). Suspended cells were then transduced with viral media for 48 h before proceeding with coculture. iRFP670 labeled receiver cells were transiently transfected with SynNotch constructs 24 h prior to coculture. Cells were added at ratios between 1:4 and 1:10 receiver cells to sender cells and cultured for 24 h before fixation in 4% paraformaldehyde.

Flow Cytometry. Cells were analyzed by flow cytometry in suspension on an Attune NxT flow cytometer (Thermo Fisher) and analyzed by FlowJo (v10). Live cells were gated by forward and side scatter detection. Of the live cells, populations were gated for being fluorescently positive if their fluorescence intensity was greater than or equal to the top 1% of nontransfected cells. For Gal4-DB-peptide and NS3-transcription effector experiments, a 1:2 molar ratio of DNA binding domain to transcriptional effector was used. A cotransfection marker of a constitutively expressed protein, mTurq2, was used, and cells were deemed positively transfected if they were mTurq2 fluorescently positive. Hereafter, the geometric mean of reporter UAS-H2B-mCherry (dNS3-VPR experiments) or UAS-CMV-H2B-Citrine (dNS3-KRAB experiments) was measured and normalized to a control.

For Cre recombinase control in mammalian cells, live cells were gated in the same manner as above and gated for transfection by either a cotransfection marker of pmiRFP670-N1 or interplasmidic constitutive expression of iRFP670 under a separate constitutive promoter. Cells were further deemed as GFP positive if their fluorescence intensity was greater than or equal to the top 1% of nontransfected cells. Baseline activation of GFP positive cells was then subtracted using transfection marker only cells as a baseline for all measurements.

Luciferase Assay. HEK293FT cells were transfected with split luciferase constructs. In the case of drug pretreatment for dose curve experiments, the drug was added at the indicated concentration at the time of transfection. Two days later, the transfected cells were lysed with 1× Ex Luciferase Assay Buffer using the Nano-Glo Dual-Luciferase Reporter Assay System (Promega). Immediately after, the samples were treated with an additional volume of 1× Ex Luciferase Assay Buffer with the indicated concentration of the drug. The samples were then read with a plate reader once per minute measuring luminescence with a 500 ms exposure time. Samples which had not been incubated in the drug had decreased luminescence over time, corresponding to utilization of the luciferase reagents. For dose response analysis, data sets were normalized using GraphPad Prism. For kinetics analysis, linear regression analysis was performed on the untreated samples and used to normalize the data for the treated samples.

Bacterial Cell Culture. *E. coli* strain BW25113 was used for all bacterial experiments. Drug inducible Cre expression plasmids were derived from the low copy (SC101) plasmid pBbS8c from Lee et al.[38] For readout of the Cre recombination, a transcriptional terminator flanked by LoxP sites was located between a constitutive promoter and the gene encoding superfolder GFP (sfGFP). The terminator is excised upon recombination, allowing transcription of sfGFP. Cells were transformed and inoculated in 3 mL of LB with 25 μg/mL of chloramphenicol and 30 μg/mL of kanamycin for Cre expression and reporter plasmid maintenance, respectively. Cells were grown at 37 °C with 200 rpm of shaking. In the case of arabinose inducible constructs (Figure S10), cultures were pretreated with 1 mM arabinose for 2 h prior to drug treatment when appropriate. Experiments were carried out in clear 96-well plates with cell cultures diluted 1:100 into a culture volume of 200 μL. OD_{600} and fluorescence were measured in a BioTek Synergy H1 plate reader after 6 h of drug treatment. For sfGFP detection, excitation and emission wavelengths of 480 and 510 nm were used, respectively.

Image Acquisition and Analysis. To prepare cells for imaging, transfected cells in ibiTreat 8-wells (iBidi) were fixed in 4% paraformaldehyde (Thermo Fisher) diluted in PBS for less than or equal to 10 min, followed by three rinses with PBS, and then quenching with 5% BSA. Fixed cells were maintained and imaged in PBS.

Images were acquired with epifluorescence using a Zeiss AxioObserver Z1 microscope and Zen software (Zeiss). Representative images were taken and processed in ImageJ-based image analysis package Fiji.

Statistics. All statistical analyses for flow cytometry were performed in Prism (v7.04) using three independent biological replicates. For imaging conditions at least three images were taken per condition, and representative images were selected. Statistical significance was determined via standard *t* tests in Excel. For temporal luciferase experiments, linear regressions were also performed in Prism (v7.04) using three independent biological replicates.

■ ASSOCIATED CONTENT

Supporting Information

The Supporting Information is available free of charge at https://pubs.acs.org/doi/10.1021/acschembio.3c00138.

Supplemental Figures 1−10, including further characterization of transcription factor systems, larger field of view images of Figure 1f, normalization curves and fitting for split luciferase data, further inducible Cre recombinase data, and toxicity of selected antiviral drugs for *E. coli*; Supplemental Tables 1 and 2, containing peptide amino acid sequences and bacterial promoter sequence information; coding region sequence information for relevant plasmids used in the manuscript (PDF)

■ AUTHOR INFORMATION

Corresponding Author

John T. Ngo − *Department of Biomedical Engineering and Biological Design Center, Boston University, Boston, Massachusetts 02215, United States;* orcid.org/0000-0003-3508-1915; Email: jtngo@bu.edu

Authors

Elliot P. Tague − *Department of Biomedical Engineering and Biological Design Center, Boston University, Boston, Massachusetts 02215, United States;* orcid.org/0000-0002-7129-5913

Jeffrey B. McMahan − *Department of Biomedical Engineering and Biological Design Center, Boston University, Boston,*

Massachusetts 02215, United States; orcid.org/0000-0001-5845-605X

Nathan Tague − *Department of Biomedical Engineering and Biological Design Center, Boston University, Boston, Massachusetts 02215, United States;* orcid.org/0000-0002-8114-6700

Mary J. Dunlop − *Department of Biomedical Engineering and Biological Design Center, Boston University, Boston, Massachusetts 02215, United States;* orcid.org/0000-0002-9261-8216

Complete contact information is available at: https://pubs.acs.org/10.1021/acschembio.3c00138

Author Contributions

E.P.T and J.T.N devised the concept and design. E.P.T, J.B.M., and N.T. performed and analyzed experiments. J.T.N. and M.J.D. supervised the work. E.P.T. and J.T.N. wrote the manuscript and prepared figures with input from J.B.M., N.T., and M.J.D.

Notes

The authors declare the following competing financial interest(s): A patent application has been filed based on this work (J.T.N, E.P.T., N.T., and M.J.D.).

■ ACKNOWLEDGMENTS

Support for this was provided through NIH research grants R35 GM128859 (to J.T.N.) and R01 HL147585 (to J.T.N.). E.P.T. was also supported through a T32 NIH Training Grant awarded to Boston University (EB006359). M.J.D. and N.T. acknowledge funding from NIH Grant R01AI102922 and DOE Grant BER DE-SC0019387. The pEV-UAS-H2B-Citrine reporter plasmid was a gift from M. Elowitz (Caltech, Pasadena, CA, USA). The Cre Reporter plasmid was a gift from N. Geijsen (Leiden University, Netherlands). The pCAG-ERT2CreERT2 plasmid was a gift from C. Cepko (Harvard University, MA, USA). We also thank Ngo lab members for suggestions on the manuscript.

■ REFERENCES

(1) Spencer, D. M.; Wandless, T. J.; Schreiber, S. L.; Crabtree, G. R. Controlling signal transduction with synthetic ligands. *Science* **1993**, *262*, 1019−1024.

(2) Trost, M.; Blattner, A. C.; Lehner, C. F. Regulated protein depletion by the auxin-inducible degradation system in Drosophila melanogaster. *Fly (Austin)*. **2016**, *10*, 35−46.

(3) Hill, Z. B.; Martinko, A. J.; Nguyen, D. P.; Wells, J. A. Human antibody-based chemically induced dimerizers for cell therapeutic applications. *Nat. Chem. Biol.* **2018**, *14*, 112−117.

(4) Liang, F.-S.; Ho, W. Q.; Crabtree, G. R. Engineering the ABA Plant stress pathway for regulation of induced proximity. *Sci. Signal.* **2011**, *4*, 1−10.

(5) Miyamoto, T.; et al. Rapid and orthogonal logic gating with a gibberellin-induced dimerization system. *Nat. Chem. Biol.* **2012**, *8*, 465−470.

(6) Boncompain, G.; et al. Synchronization of secretory protein traffic in populations of cells. *Nat. Methods* **2012**, *9*, 493−498.

(7) Matsuda, T.; Cepko, C. L. Controlled expression of transgenes introduced by in vivo electroporation. *Proc. Natl. Acad. Sci. U.S.A.* **2007**, *104*, 1027−1032.

(8) Tague, E. P.; Dotson, H. L.; Tunney, S. N.; Sloas, D. C.; Ngo, J. T. Chemogenetic control of gene expression and cell signaling with antiviral drugs. *Nat. Methods* **2018**, *15*, 519−522.

(9) Jacobs, C. L.; Badiee, R. K.; Lin, M. Z. StaPLs: Versatile genetically encoded modules for engineering drug-inducible proteins. *Nat. Methods* **2018**, *15*, 523−526.

(10) Nishikawa, F.; et al. Inhibition of HCV NS3 protease by RNA aptamers in cells. *Nucleic Acids Res.* **2003**, *31*, 1935−1943.

(11) Kügler, J.; et al. High affinity peptide inhibitors of the hepatitis C virus NS3−4A protease refractory to common resistant mutants. *J. Biol. Chem.* **2012**, *287*, 39224−39232.

(12) Zhang, W.; et al. Optogenetic control with a photocleavable protein, Phocl. *Nat. Methods* **2017**, *14*, 391−394.

(13) Cunningham-Bryant, D.; Dieter, E. M.; Foight, G. W.; Rose, J. C.; Loutey, D. E.; Maly, D. J. A Chemically Disrupted Proximity System for Controlling Dynamic Cellular Processes. *J. Am. Chem. Soc.* **2019**, *141*, 3352−3355.

(14) Foight, G. W.; et al. Multi-input chemical control of protein dimerization for programming graded cellular responses. *Nat. Biotechnol.* **2019**, *37*, 1209−1216.

(15) Li, H.-S.; Wong, N. M.; Tague, E.; Ngo, J. T.; Khalil, A. S.; Wong, W. W. High-performance multiplex drug-gated CAR circuits. *Cancer Cell* **2022**, *40*, 1294−1305.e4.

(16) Zhang, R.; et al. Probing the substrate specificity of hepatitis C virus NS3 serine protease by using synthetic peptides. *J. Virol* **1997**, *71*, 6208−6213.

(17) Li, K.; et al. Immune evasion by hepatitis C virus NS3/4A protease-mediated cleavage of the Toll-like receptor 3 adaptor protein TRIF. *Proc. Natl. Acad. Sci. U. S. A.* **2005**, *102*, 2992−2997.

(18) Li, X.-D.; Sun, L.; Seth, R. B.; Pineda, G.; Chen, Z. J. Hepatitis C virus protease NS3/4A cleaves mitochondrial antiviral signaling protein off the mitochondria to evade innate immunity. *Proc. Natl. Acad. Sci. U. S. A.* **2005**, *102*, 17717−17722.

(19) Pethe, M. A.; Rubenstein, A. B.; Khare, S. D. Large-Scale Structure-Based Prediction and Identification of Novel Protease Substrates Using Computational Protein Design. *J. Mol. Biol.* **2017**, *429*, 220−236.

(20) Chavez, A.; et al. Highly efficient Cas9-mediated transcriptional programming. *Nat. Methods* **2015**, *12*, 326−8.

(21) DelRosso, N.; et al. Large-scale mapping and systematic mutagenesis of human transcriptional effector domains. *Nature* **2023**, *616*, 365−372.

(22) Morsut, L.; et al. Engineering Customized Cell Sensing and Response Behaviors Using Synthetic Notch Receptors. *Cell* **2016**, *164*, 780−791.

(23) Roybal, K. T.; et al. Precision Tumor Recognition by T Cells with Combinatorial Antigen-Sensing Circuits. *Cell* **2016**, *164*, 770−779.

(24) Luker, K. E.; et al. Kinetics of regulated protein-protein interactions revealed with firefly luciferase complementation imaging in cells and living animals. *Proc. Natl. Acad. Sci. U. S. A.* **2004**, *101*, 12288−12293.

(25) Perni, R. B.; et al. Preclinical profile of VX-950, a potent, selective, and orally bioavailable inhibitor of hepatitis C virus NS3−4A serine protease. *Antimicrob. Agents Chemother.* **2006**, *50*, 899−909.

(26) Hagel, M.; et al. Selective irreversible inhibition of a protease by targeting a noncatalytic cysteine. *Nat. Chem. Biol.* **2011**, *7*, 22−24.

(27) Weinberg, B. H.; Cho, J. H.; Agarwal, Y.; Pham, N. T. H.; Caraballo, L. D.; Walkosz, M.; Ortega, C.; Trexler, M.; Tague, N.; Law, B.; Benman, W. K. J.; Letendre, J.; Beal, J.; Wong, W. W. High-performance chemical and light-inducible recombinases in mammalian cells and mice. *Nat. Commun.* **2019**, *10*, 1−10.

(28) Martin, S. S.; Chu, V. C.; Baldwin, E. Modulation of the active complex assembly and turnover rate by protein-DNA interactions in Cre-LoxP recombination. *Biochemistry* **2003**, *42*, 6814−6826.

(29) Serre, M. C.; et al. The Carboxy-Terminal αN Helix of the Archaeal XerA Tyrosine Recombinase Is a Molecular Switch to Control Site-Specific Recombination. *PLoS One* **2013**, *8*, e63010.

(30) Unnikrishnan, A.; Amero, C.; Yadav, D. K.; Stachowski, K.; Potter, D.; Foster, M. P. DNA binding induces a cis -to- trans switch in Cre recombinase to enable intasome assembly. *Proc. Natl. Acad. Sci. U. S. A.* **2020**, *117*, 24849−24858.

(31) Guo, F.; Gopaul, D. N.; Van Duyne, G. D. Structure of Cre recombinase complexed with DNA in a site-specific recombination synapse. *Nature* **1997**, *389*, 40−46.
(32) Ringrose, L.; et al. Comparative kinetic analysis of FLP and Cre recombinases: Mathematical models for DNA binding and recombination. *J. Mol. Biol.* **1998**, *284*, 363−384.
(33) Eroshenko, N.; Church, G. M. Mutants of Cre recombinase with improved accuracy. *Nat. Commun.* **2013**, *4*, 2509.
(34) Duplus-Bottin, H.; Spichty, M.; Triqueneaux, G.; Place, C.; Mangeot, P. E.; Ohlmann, T.; Vittoz, F.; Yvert, G. A single-chain and fast-responding light-inducible cre recombinase as a novel optogenetic switch. *Elife* **2021**, *10*, 1−52.
(35) Dickinson, B. C.; Packer, M. S.; Badran, A. H.; Liu, D. R. A system for the continuous directed evolution of proteases rapidly reveals drug-resistance mutations. *Nat. Commun.* **2014**, *5*, 5352.
(36) Pu, J.; Chronis, I.; Ahn, D.; Dickinson, B. C. A Panel of Protease-Responsive RNA Polymerases Respond to Biochemical Signals by Production of Defined RNA Outputs in Live Cells. *J. Am. Chem. Soc.* **2015**, *137*, 15996−15999.
(37) de Wispelaere, M.; Du, G.; Donovan, K. A.; Zhang, T.; Eleuteri, N. A.; Yuan, J. C.; Kalabathula, J.; Nowak, R.ła. P.; Fischer, E. S.; Gray, N. S.; Yang, P. L. Small molecule degraders of the hepatitis C virus protease reduce susceptibility to resistance mutations. *Nat. Commun.* **2019**, *10*, 3468.
(38) Lee, T. S.; Krupa, R. A; Zhang, F.; Hajimorad, M.; Holtz, W. J; Prasad, N.; Lee, S. K.; Keasling, J. D BglBrick vectors and datasheets: A synthetic biology platform for gene expression. *J. Biol. Eng.* **2011**, *5*, 15−17.

https://doi.org/10.1021/acschembio.3c00138
ACS Chem. Biol. 2023, 18, 1228−1236